Characterization of Multilayer Diffractors for Framed Monochromatic Imaging

Archana Venkataraman

Characterization of Multilayer Diffractors for Framed Monochromatic Imaging

Archana Venkataraman
University of Rochester, Laboratory for Laser Energetics
2002 Summer High School Program

INTRODUCTION

The OMEGA laser facility[1] at the University of Rochester's Laboratory for Laser Energetics is used to explore the conditions needed for sustaining thermonuclear fusion reactions[2]. X rays emitted by the laser-generated plasma can be imaged, providing information about the state of the plasma, i.e. temperature and density. Framing cameras allow the x-ray emission to be resolved in time and, when used in combination with mirrors and filters, to image the emission in narrow energy bands[3].

In this work, two WB_4C (tungsten boron carbide) multilayers[4] are characterized at several x-ray energies by finding the efficiency (reflectivity) of each one as a function of angle. A Gaussian analysis of this data yields values of the peak reflectivity and the energy resolution [full width at half maximum (FWHM)]. Analysis of multiple energies allows for inference of the atomic layer spacing d. The multilayers which have nominal layer spacings of 26 Å and 37Å are found to have reflectivities of ~40 to ~70 % and ~32 to ~89 % respectively and narrow energy resolutions of 1.5 to 2.1 % and 1.8 to 3.7 % respectively. Both are functions of energy. When used in conjunction with framing cameras on the OMEGA laser, they will provide time-resolved, narrow energy band (monochromatic) images of the laser-plasma x-ray emission.

EXPERIMENTS

This project entails the calibration of two such WB_4C multilayer diffractors with approximate 2d atomic layer spacings of 26 and 37 Å to be used in the study of laser fusion plasmas. There are three properties of each multilayer that must be determined. The first is the layer spacing d, the second is the reflectivity as a function of energy, and the third is the energy resolution. This is accomplished by measuring x rays diffracted from the multilayer as a function of angle for three emission lines using a Si PIN detector[5]. By finding the angle of maximum reflectivity, or Bragg angle, these characteristics can be determined by using the following derivation[6]:

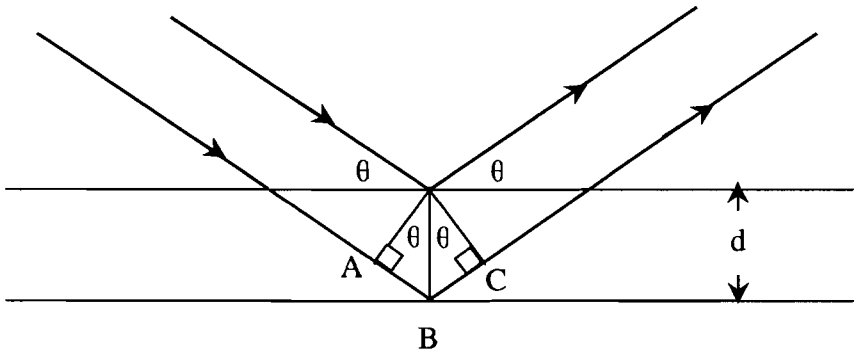

Path difference = AB + BC = $d \sin\theta + d \sin\theta$

If the path difference is an integral number of wavelengths the outgoing waves interfere constructively, hence

$$n\lambda = 2d \sin\theta, \tag{1}$$

where λ is the wavelength, d is the layer spacing, and θ is the angle the ray makes with the tangent to the surface.

(a) BEAM COLLIMATION AND ALIGNMENT

The x-ray source must be collimated to observe the desired diffraction. The collimator consists of two slits, aligned optically using a telescope, restricting the x-ray emission to a narrow beam. The entrance aperture (dimensions 0.175 mm x 1mm) is positioned 1650 mm away from the exit aperture (dimensions 0.1 mm x 1.2 mm). The detector is positioned an additional 263 mm away from the exit aperture. Figure 1 below illustrates the final calculations of the beam size. The distance x is found using Eq. (2), Y3 is then found using Eq. (3), and then the angle α from Eq. (4).

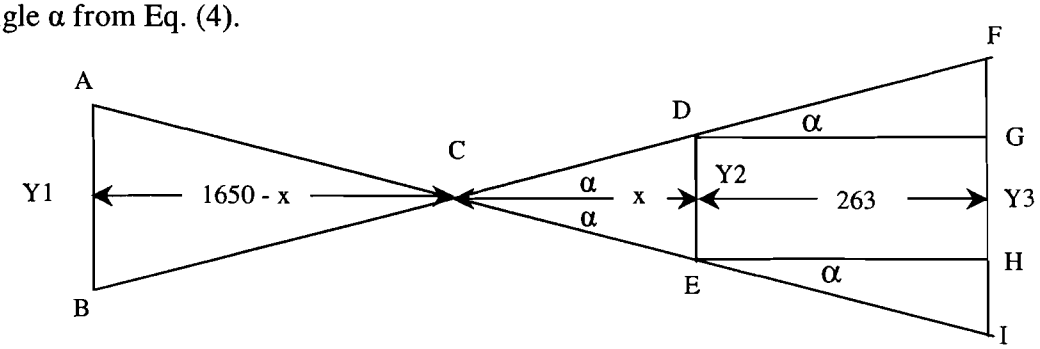

Fig. 1. Diagram of the Collimator setup followed by the calculations for the spatial and angular width of the beam

$$\frac{Y1}{1650 - x} = \frac{Y2}{x} \tag{2}$$

$$\frac{Y2}{x} = \frac{Y3}{x + 263} \tag{3}$$

$$\alpha = \tan^{-1}\left(\frac{0.5(Y3)}{x + 263}\right) \tag{4}$$

When solved using the known dimensions for the slits, the beam size is found to be 0.144 mm x 1.55 mm, making the angular width along the narrower dimension equal to 0.0096°.

Optimum beam alignment consists of the diffractor being positioned parallel to the line of sight and midway through the x-ray beam with respect to the horizontal plane. The observed

beam flux (count rate) is determined with respect to the following four values: the vertical (z) position of the detector, the horizontal (y) position of the detector, the angular orientation of the diffractor, and the horizontal (y) position of the diffractor. The adjustments are done using two concentric stepper-motor driven rotary stages mounted on a linear stage. Each step of the rotary motors equals 0.01°, and each step of the linear motor equals 2.54μm. Figure 2(a-e) below illustrate the steps of the alignment process.

Figure 2. X-ray detector alignment.

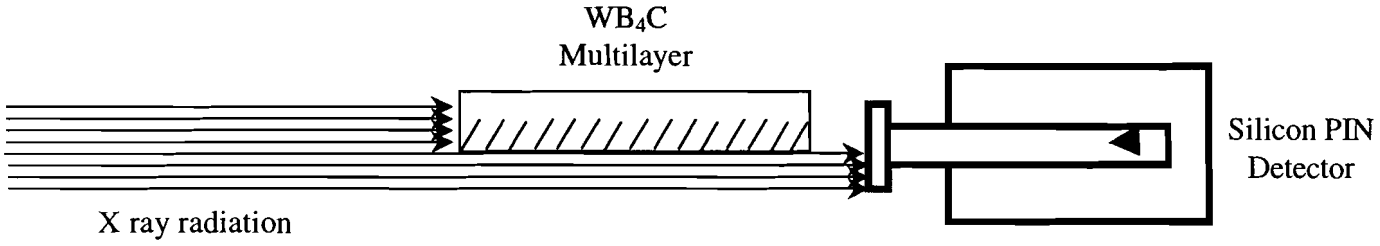

Fig. 2(a). **Alignment goal is to have diffractor parallel to beam and in its center.**

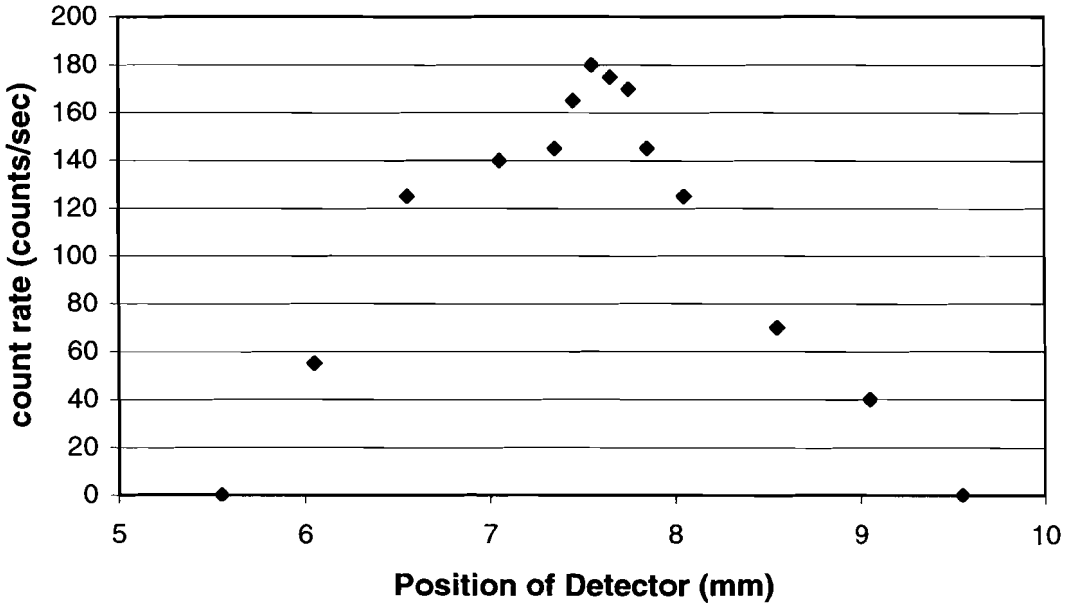

Fig. 2(b). **Count rate as a function of detector vertical position.**

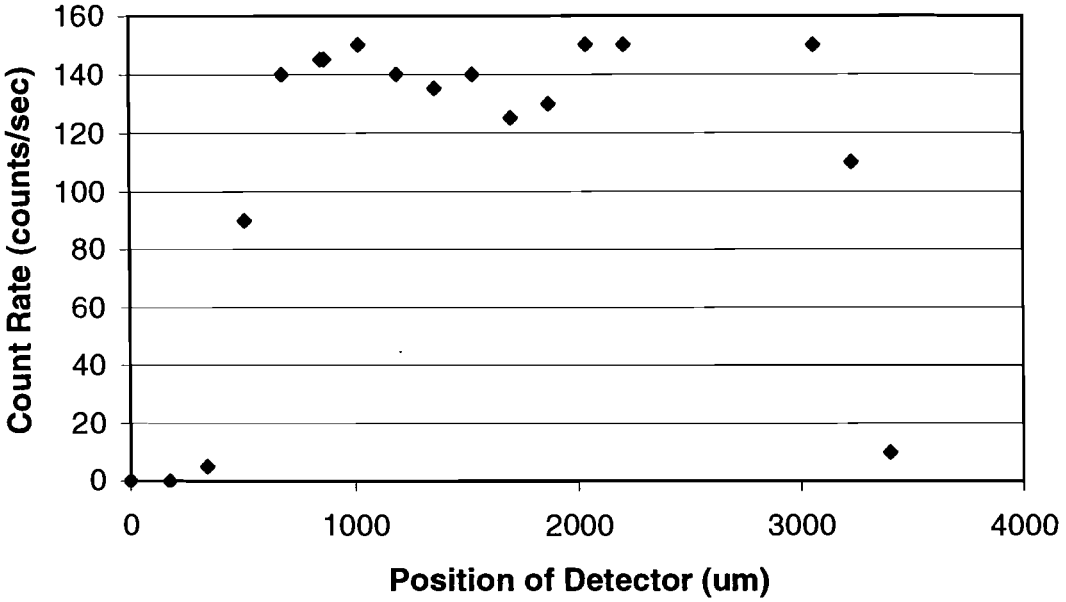

Fig. 2(c). **Count rate as a function of detector horizontal position.**

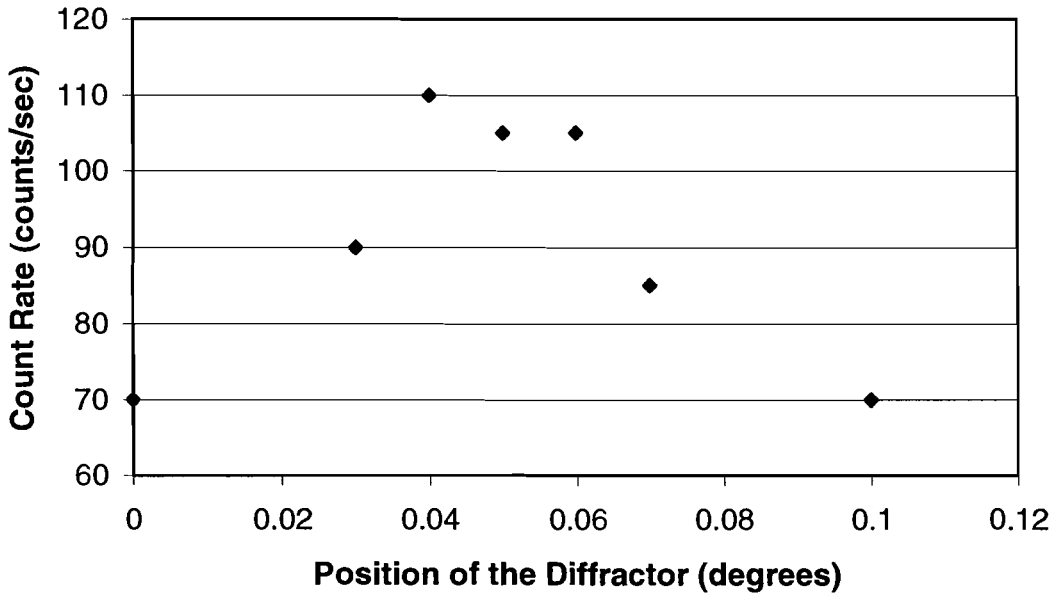

Fig. 2(d). **Count rate as a function of diffractor angular position. A maximum rate indicates that diffractor is parallel to the beam**

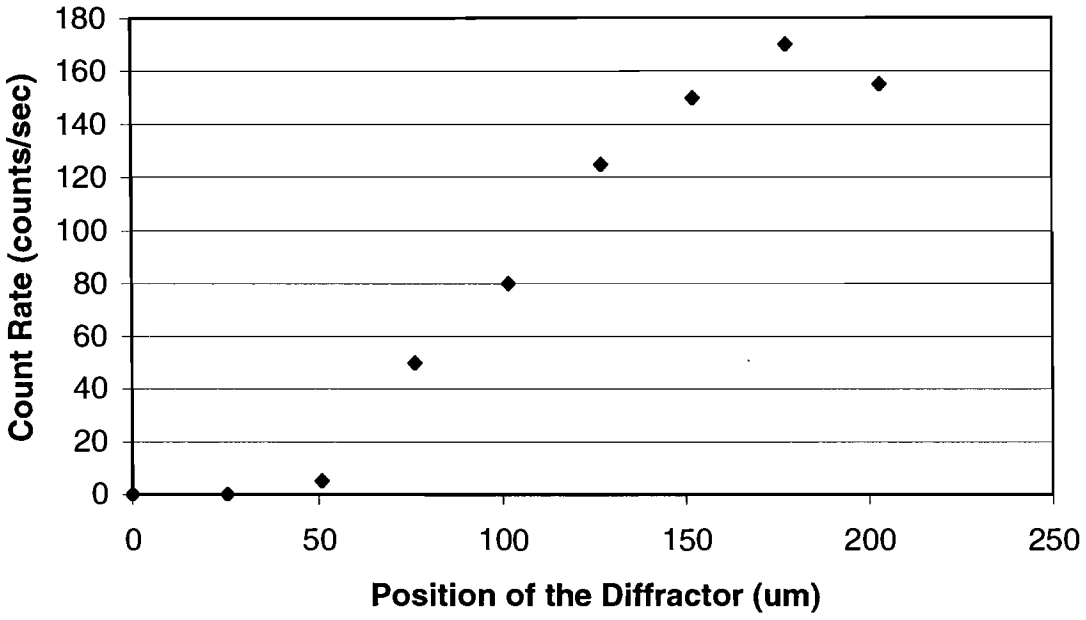

Fig. 2(e). **Count rate as a function of diffractor horizontal position.**

(b) THE X-RAY SOURCE

The source generates x rays by focusing an electron beam on a metal target[7]. By choosing the target material, different output spectra can be produced. An initial measurement of the undiffracted spectrum is taken for each target as well as subsequent readings periodically throughout the experiment. This allows for the determination of the x-ray photon flux to serve as a reference for measuring the reflectivity. Sample spectra readings for Ti, Cu and Si targets are shown in Figs. 3(a-c).

Fig 3 (a-c): Plots of undiffracted x-ray source spectra as measured by the Si PIN detector.

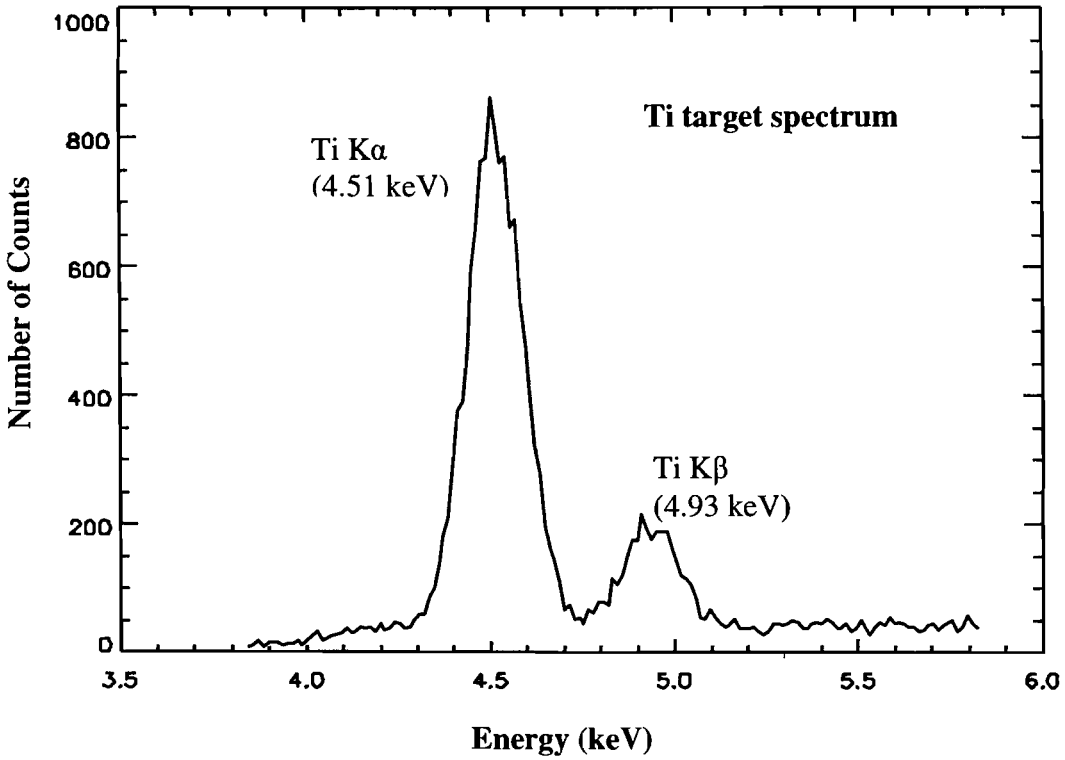

Fig. 3(a)

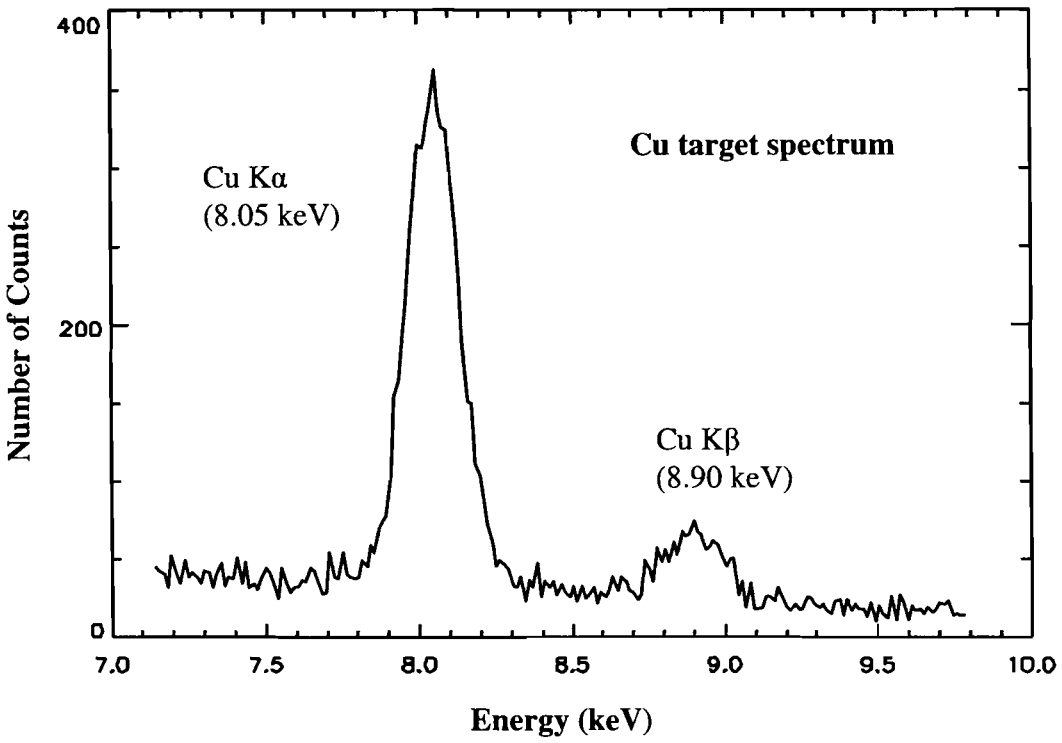
Cu target spectrum
Cu Kα
(8.05 keV)
Cu Kβ
(8.90 keV)
Number of Counts
Energy (keV)
400
200
0
7.0
7.5
8.0
8.5
9.0
9.5
10.0

Fig. 3(b)

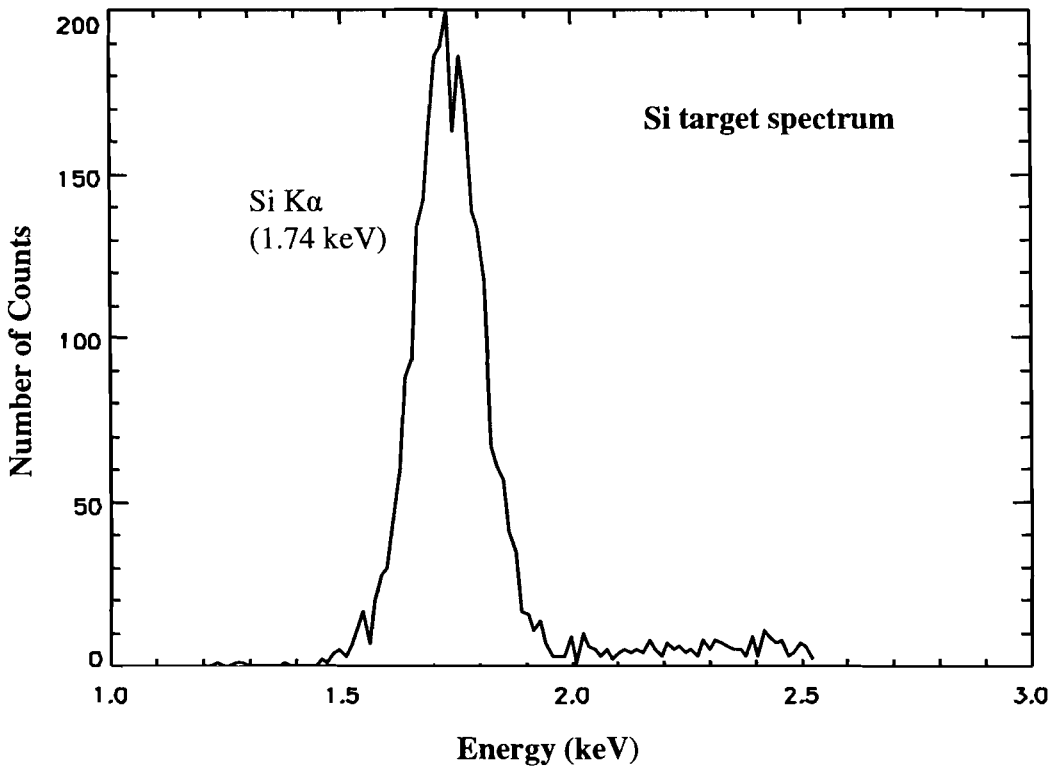
Si target spectrum
Si Kα
(1.74 keV)
Number of Counts
Energy (keV)
200
150
100
50
0
1.0
1.5
2.0
2.5
3.0

Fig. 3(c)

(c) DIFFRACTION MEASUREMENTS

In order to measure the x-ray diffraction properties of the multilayer, a scan about the Bragg angle is performed. The stepper motors are used to rotate both the multilayer and the Si PIN detector in order to locate the optimum angle of diffraction as defined by Bragg's law. The first multilayer has a nominal d spacing of 25.9 Å and is tested using the Ti Kα, Ti Kβ, and Cu Kα line emission. The second multilayer has a nominal d spacing of 37.3 Å and is tested using Si Kα, Ti Kα, and Cu Kα line emission. Figure 4 illustrates this procedure, and Figs. 5(a,b) show the diffracted peaks for each line of the first and second multilayer.

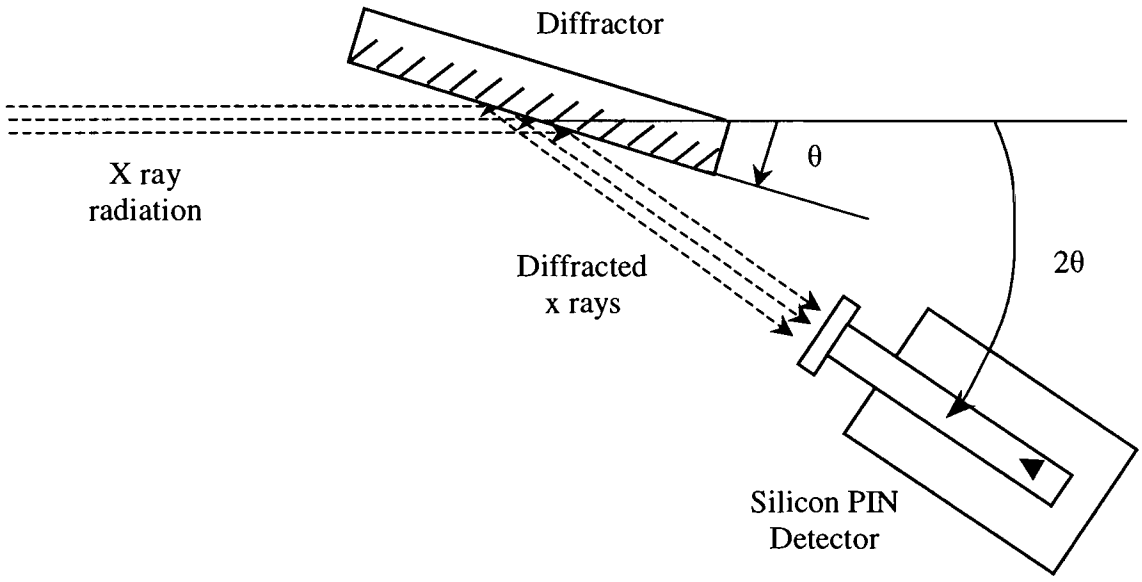

Fig. 4. Diagram of x-ray diffraction apparatus. The diffractor is positioned at an angle θ, and the detector at an angle 2θ, both of which are changed in fixed increments in order to complete the scan. Spectral data readings to check for beam fluctuations are also taken periodically throughout the procedure.

Fig. 5. Plots of each diffracted line (shown combined in this figure) at the specified angle as taken using the Si PIN detector while using both the first multilayer (a) and the second multilayer (b). The number of counts is plotted as a function of energy, but is not proportional to the reflectivity since each line measurement is taken under different conditions relative to the source.

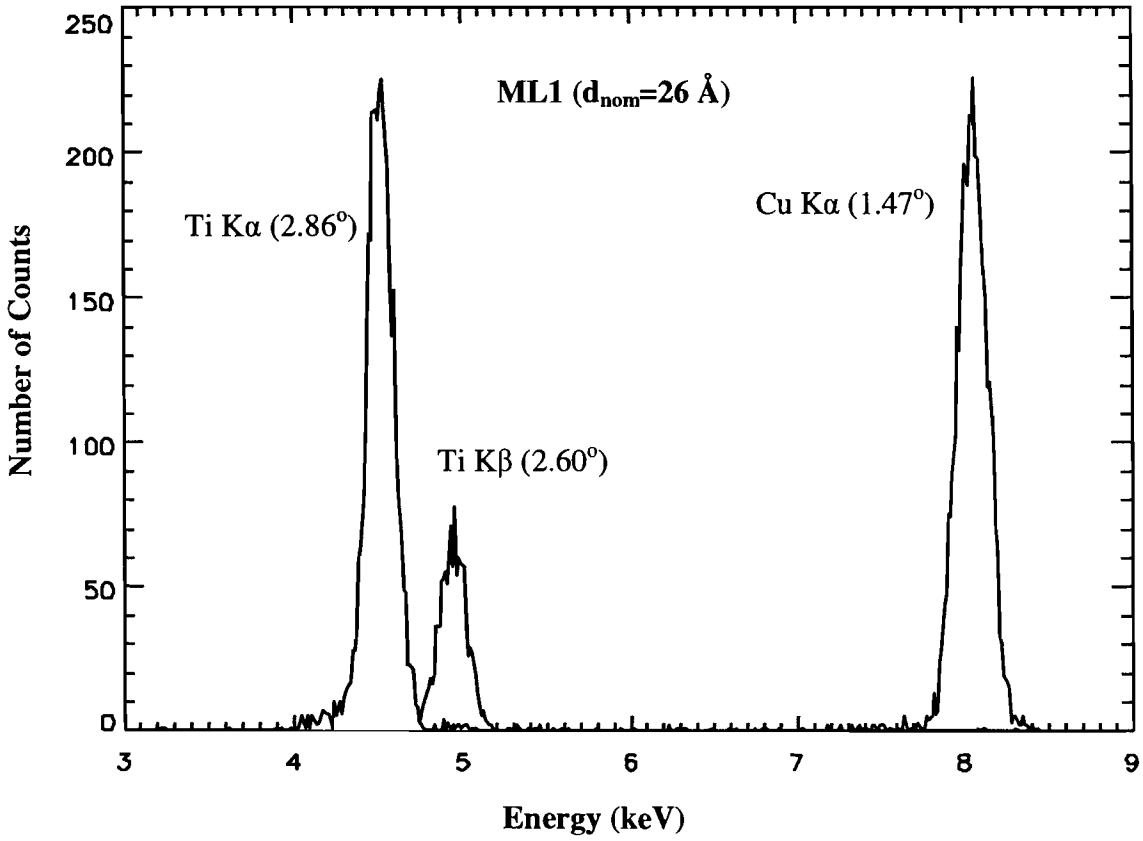

Fig. 5(a)

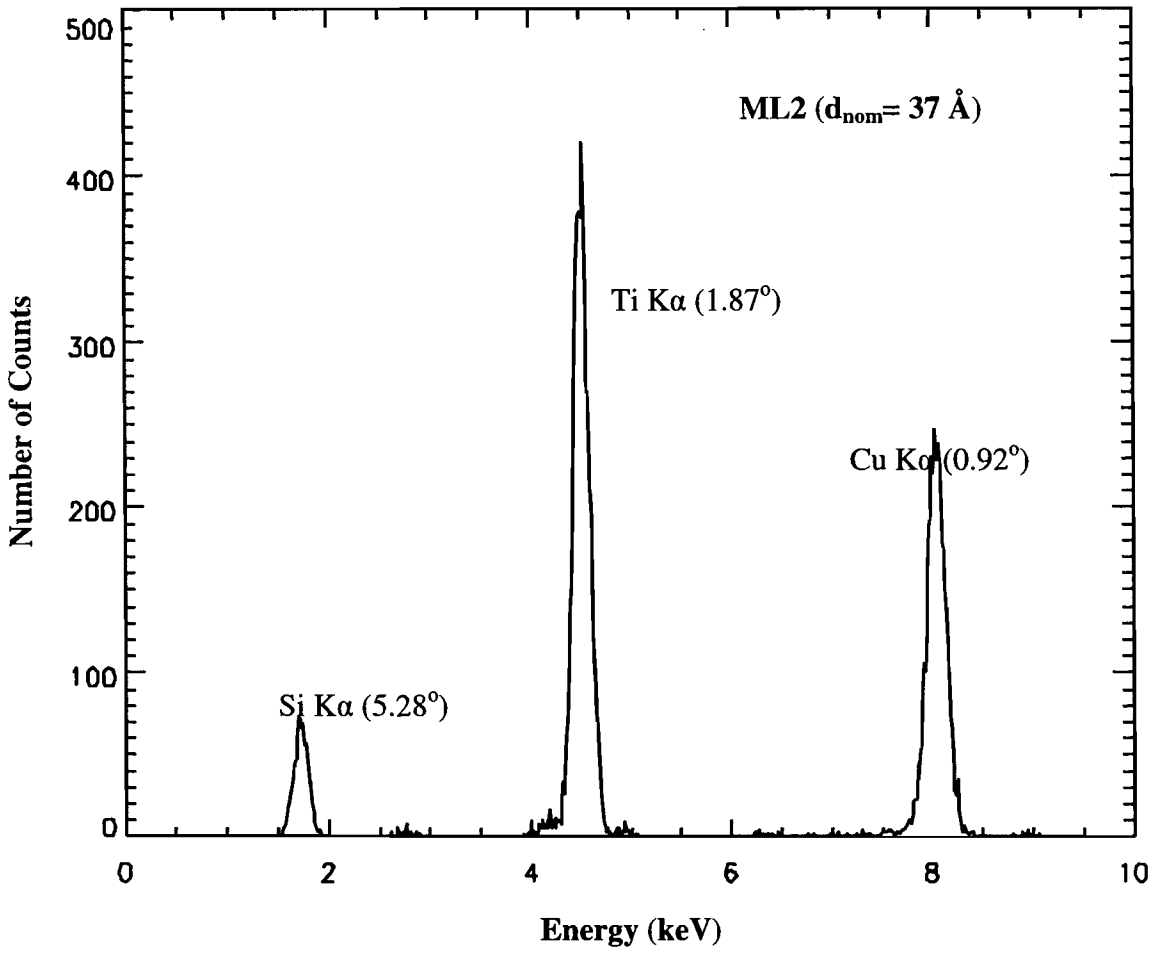

Fig. 5(b)

RESULTS

The line and spectral readings of figs. 3 and 5 taken by the detector displayed the results in terms of counts per bin where each bin corresponds to a mean photon energy. The energy axis scaling factor is calibrated using an Fe^{55} source[8] and fitted to a Gaussian distribution as follows[9]:

$$f(x) = \frac{1}{\sqrt{2\pi}\,\sigma} e^{-\frac{(x - x_m)^2}{2\sigma^2}} \tag{5}$$

where x is the angular position, and x_m is the position of the peak, and σ is the standard deviation in degrees. The optimization is done using the CURVEFIT program in PV Wave[10,11].

The reflectivity at a given x-ray line energy is determined by dividing the diffracted x-ray count rate by the undiffracted count rate from the same line. The x-ray source rate is monitored periodically to establish its rate as a function of time. The reflectivity is then plotted as a function of angle, and another Gaussian fit is applied in order to determine the angle at which there is a maximum reflectivity.

The integrated reflectivity R_{int} is taken to be the area under the fitted Gaussian and is given by:

$$R_{int} = R_P \sigma \sqrt{\pi}, \tag{6}$$

where R_{int} is in units of degrees, R_P is the peak reflectivity, and σ is the standard deviation. The FWHM of each Gaussian is equal to 2.35σ. Table 1 and Fig. 6 summarize the results gathered when plotting this final result to obtain the maximum angle and reflectivity.

	(a)	(b)	(c)	(d)	(e)	(f)	(g)	(h)	(i)	(j)
Multilayer	Line	Energy	λ	θ_B	R_p	R_{int}	FWHM	b_k	error θ_B	$\frac{\Delta E}{E}$
		(keV)	(Å)	(deg)		(deg)	(deg)		(deg)	
1	Ti Kα	4.51	2.75	2.860	0.395	0.0132	0.044	0.042	0.00215	0.015
	Ti Kβ	4.93	2.51	2.603	0.427	0.0159	0.050	0.061	0.00194	0.019
	Cu Kα	8.05	1.54	1.475	0.690	0.0160	0.031	0.037	0.00104	0.021
2	Si Kα	1.74	7.13	5.292	0.323	0.0237	0.097	0.038	0.00460	0.018
	Ti Kα	4.51	2.75	1.888	0.542	0.0230	0.056	0.035	0.00310	0.030
	Cu Kα	8.05	1.54	0.911	0.888	0.0223	0.033	0.029	0.00052	0.037

Table 1: Measured Properties of WB_4C Multilayer Diffractors. (a) Line name, (b) Line energy in keV, (c) Line wavelength in Å, (d) Bragg angle in degrees, (e) Peak reflectivity, (f) Integrated reflectivity in degrees, (g) Full Width at Half Maximum in degrees, (h) Constant background of reflectivity curve, (i) One standard deviation of the Bragg angle, (j) Energy Resolution.

Fig 6: Measured diffraction efficiency (reflectivity). WB_4C multilayer # 1 (a-c), and WB_4C multilayer # 2 (d-f).

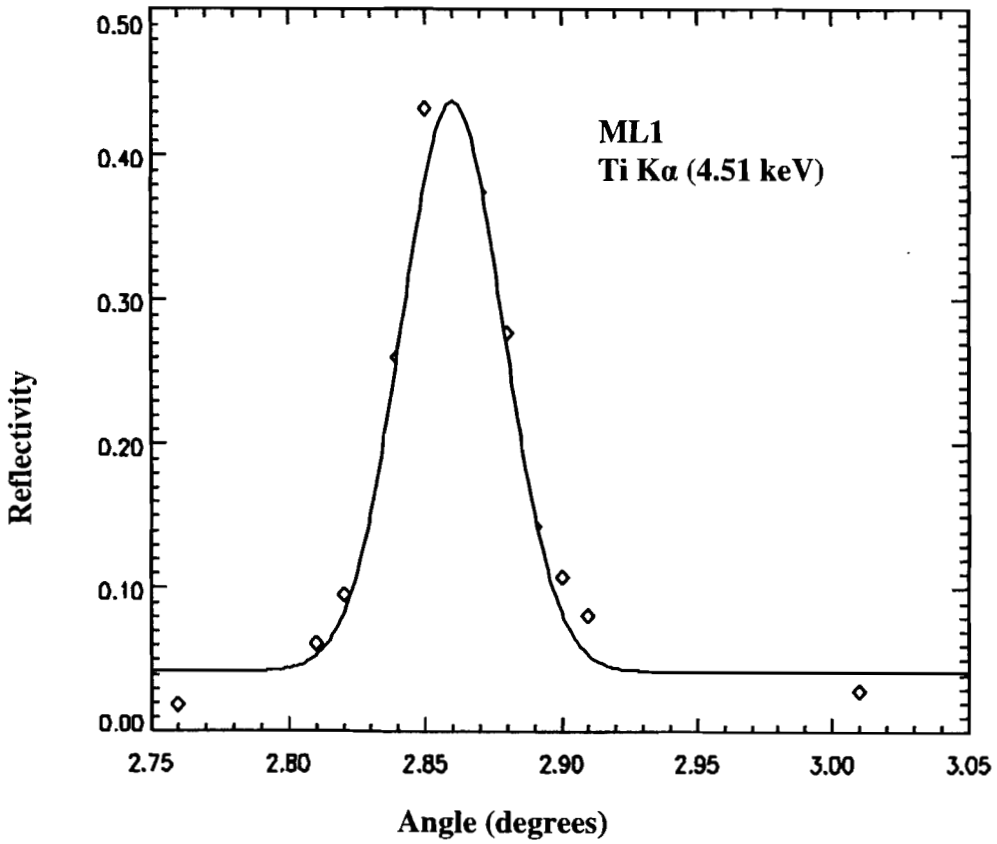

Fig. 6(a)

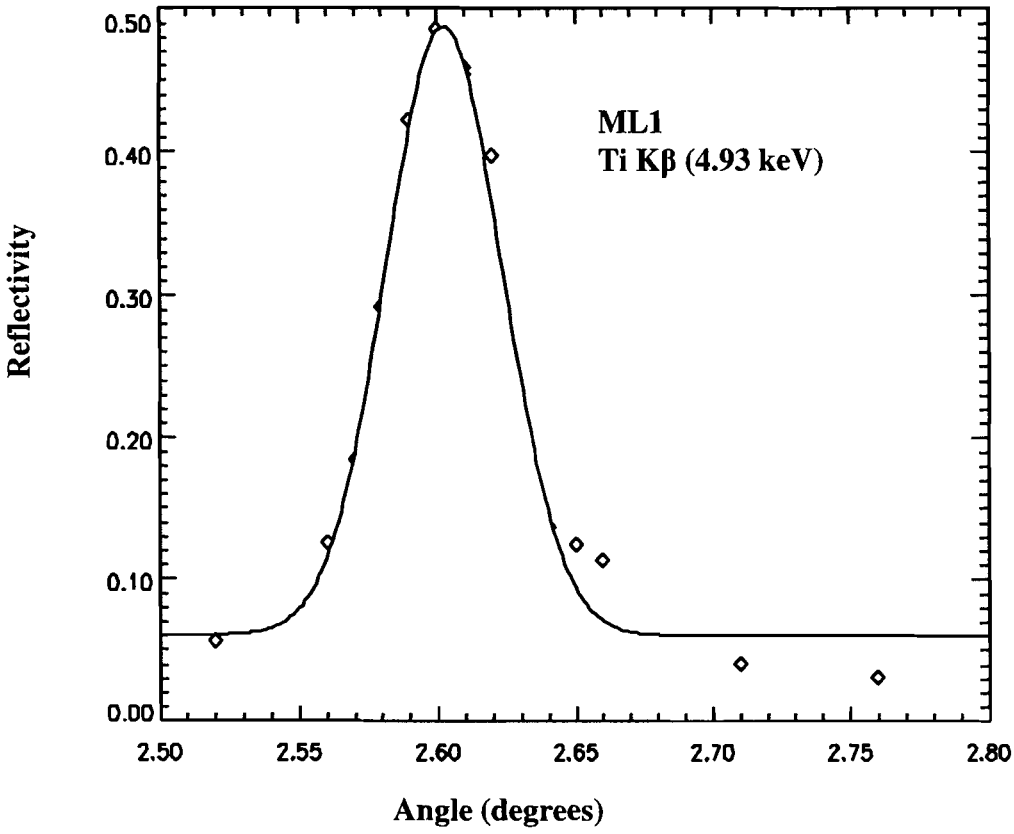
ML1
Ti Kβ (4.93 keV)
Reflectivity
0.50
0.40
0.30
0.20
0.10
0.00
2.50
2.55
2.60
2.65
2.70
2.75
2.80
Angle (degrees)

Fig. 6(b)

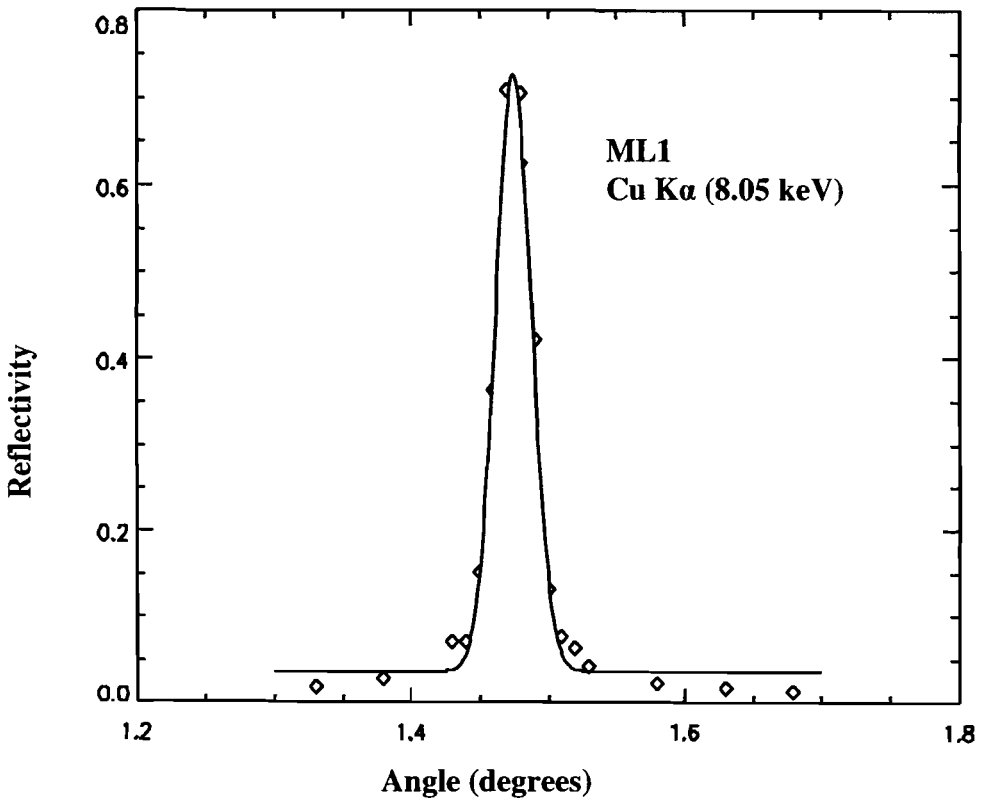
ML1
Cu Kα (8.05 keV)
Reflectivity
Angle (degrees)
0.0
0.2
0.4
0.6
0.8
1.2
1.4
1.6
1.8

Fig. 6(c)

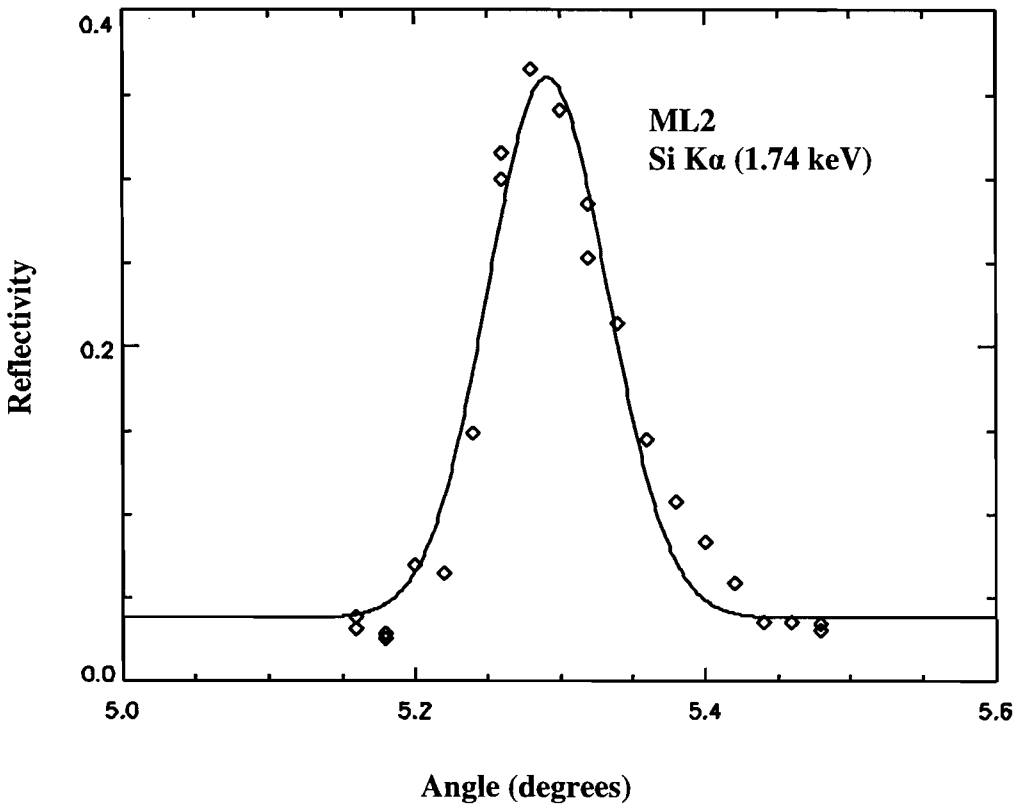
ML2
Si Kα (1.74 keV)
Reflectivity
0.4
0.2
0.0
5.0
5.2
5.4
5.6
Angle (degrees)

Fig. 6(d)

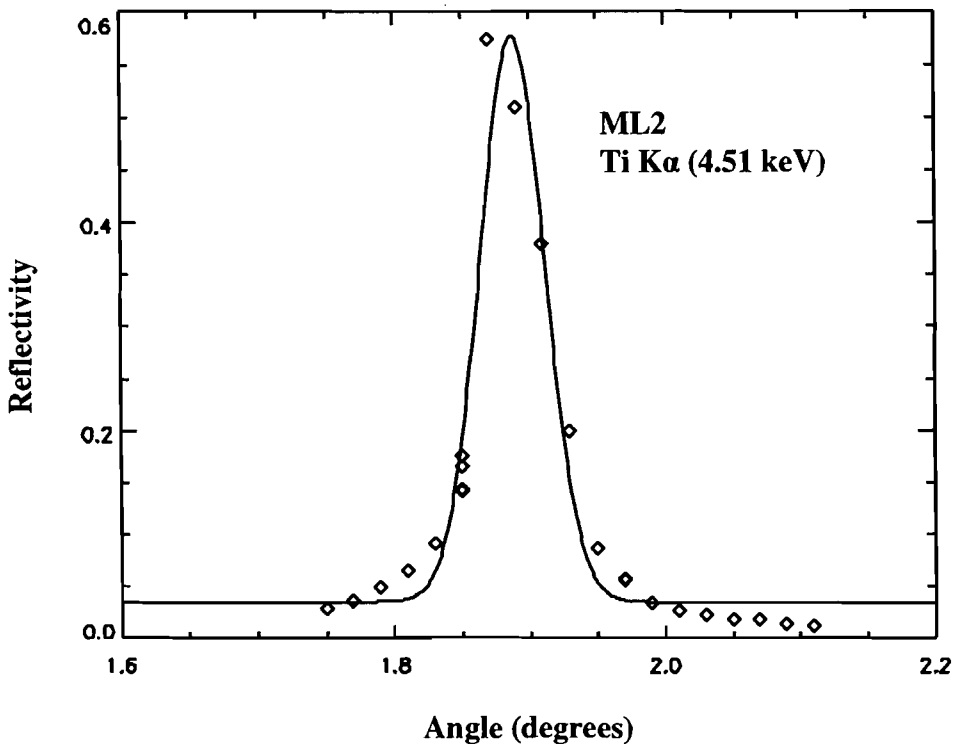
ML2
Ti Kα (4.51 keV)
Reflectivity
0.0
0.2
0.4
0.6
1.6
1.8
2.0
2.2
Angle (degrees)

Fig. 6(e)

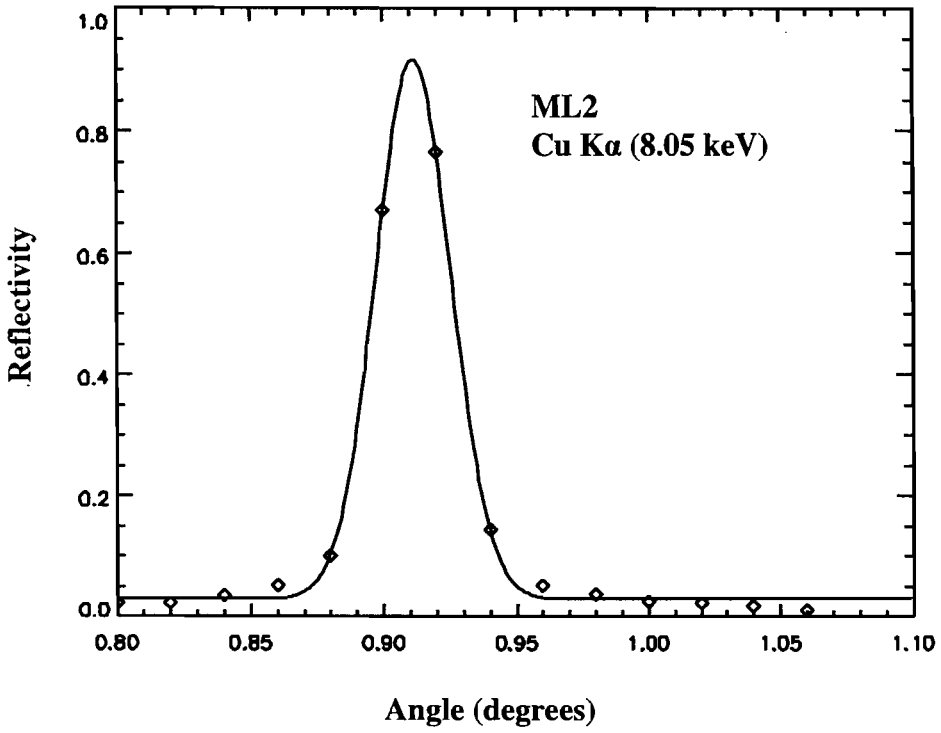
ML2
Cu Kα (8.05 keV)
Reflectivity
Angle (degrees)
1.0
0.8
0.6
0.4
0.2
0.0
0.80
0.85
0.90
0.95
1.00
1.05
1.10

Fig. 6(f)

To solve for the d spacing of each multilayer, the diffraction from more than one x ray line must be measured in order to eliminate error in the zero position. This is accomplished by solving the following equation for two or more diffracted lines:

$$\lambda_i = 2\mathrm{d}\sin(\theta_i + \theta_0) \tag{7}$$

where λ_i is the corresponding wavelength for each trial, θ_i is the measured angle of peak reflectivity, and θ_0 is the zero offset. The solution to equation 7 is obtained implicitly through graphical analysis. Equation 7 can be rewritten as follows:

$$\theta_0 = \sin^{-1}\left(\frac{\lambda_i}{2\mathrm{d}}\right) - \theta_i \tag{8}$$

The error on the best-fit value of the angle of peak reflectivity has been determined by the following prescription given in Lampton et al[12]. It is as follows: Normalize χ^2 to be equal to 1 per degree of freedom ν,

$$\frac{\chi^2}{\nu} = 1 = \frac{1}{\nu}\sum_{i=1}^{n}\left(f(a_i) - y_i\right)^2 w^2, \tag{9}$$

where $f(a_i)$ is a Gaussian fit to the observed values of reflectivity y_i, and w is chosen to make $\frac{\chi^2}{\nu} = 1$. Then select a value of the peak angle that increases χ^2 by 4.7 (appropriate for fitting four important parameters). The difference in peak angle from χ^2 minimum is an estimate of the uncertainty. Including the standard deviation fails to yield an intersection point for all three lines of each trial, indicating that there may have been additional, unaccounted errors. Alternatively, the positioning error should be no less than one step of the rotary motors (0.01°). Estimates of the error are shown in Fig 7.

Fig 7 (a-b): Implicit graphical solution to solve for the d spacing and angle offset of the first (a) and second (b) multilayer while incorporating an error of ± 0.01°.

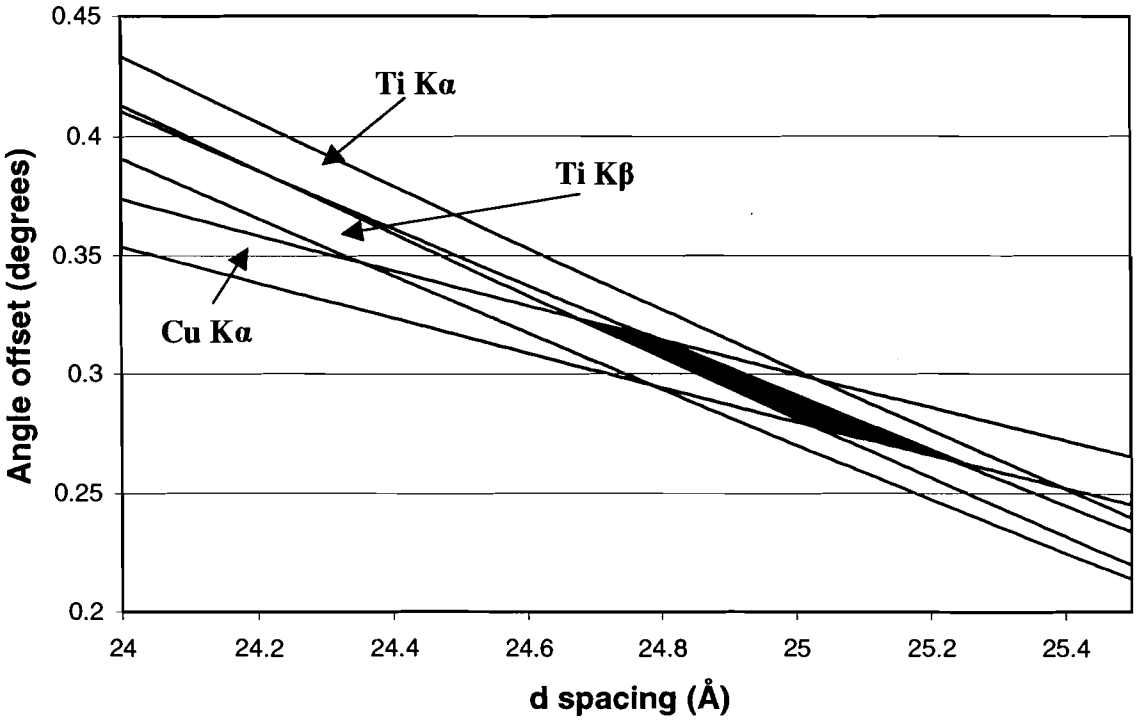

Fig. 7(a). **Angle offset as a function of d spacing for the first multilayer**

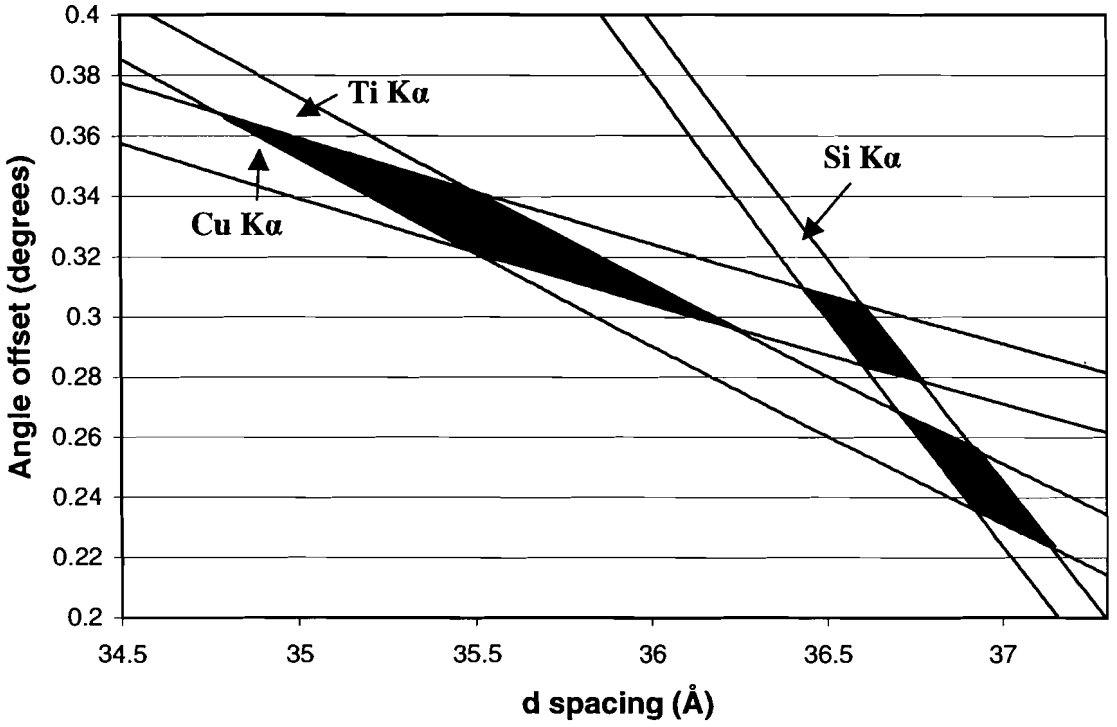

Fig. 7(b). **Angle offset as a function of d spacing for the second multilayer**

In Fig. 7(a), the intersection of the error bands for the three lines indicates the range of values for the d spacing and angle offset. Statistical analysis of the data yields a value of 24.95 ± 0.3 Å for the value of the d spacing for multilayer 1 (the midpoint of the banded region plus or minus half the length of the region). Figure 7(b) fails to yield an intersection for the three lines. Statistical analysis of the three intersections yield a value for the d spacing of 36.3 ± 0.74 Å for multilayer 2 (the average of the intersections plus or minus half the range of values within all three intersections).

The peak reflectivity of the multilayer diffractors is found to depend upon the energy of the diffracted line. This can be seen in Fig. 8 below.

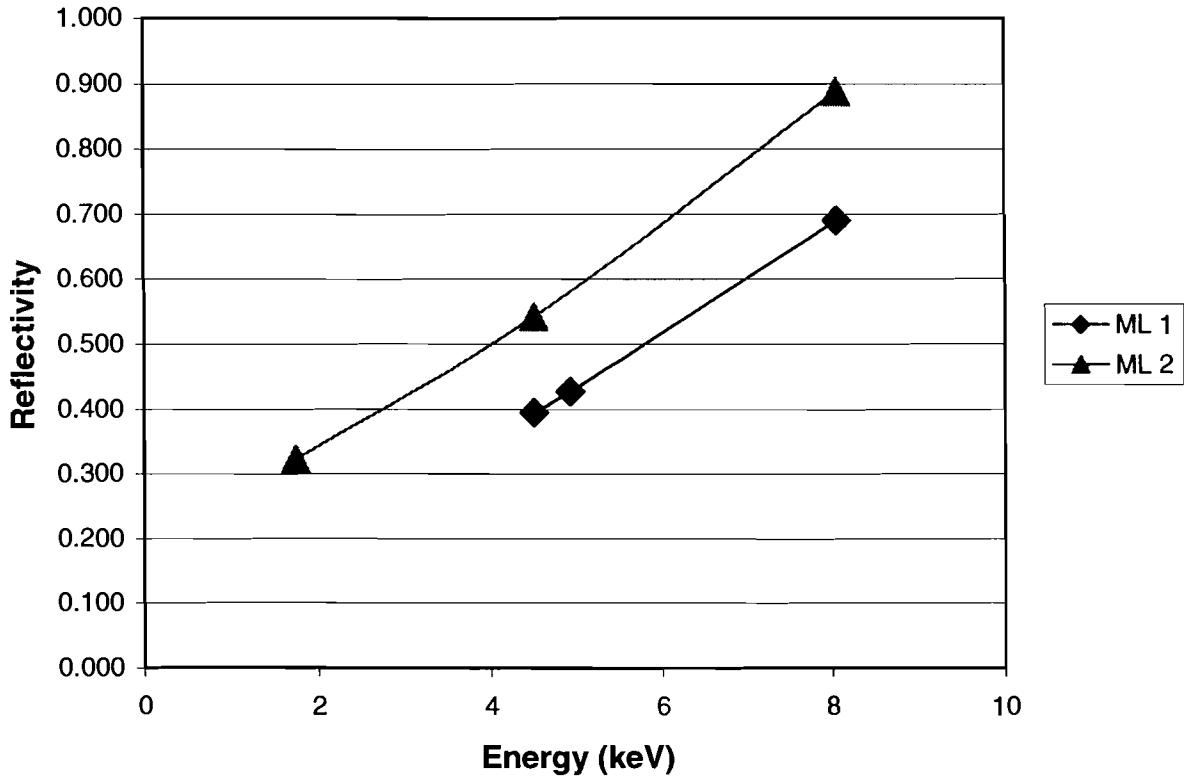

Fig. 8. Peak reflectivity as a function of energy for each multilayer

The energy response of the multilayer is defined to be $\frac{\Delta E}{E}$. Differentiating Eq. (1), and using the identity $E = hc/\lambda$, where h is Planck's constant and c is the speed of light, yields the equation

$$\frac{\Delta E}{E} = \frac{\Delta \lambda}{\lambda} = \cot(\theta)\Delta\theta, \tag{10}$$

where θ is the Bragg angle and $\Delta\theta$ is equal to the full width at half maximum. Applying the equation to the results is shown in Fig. 9.

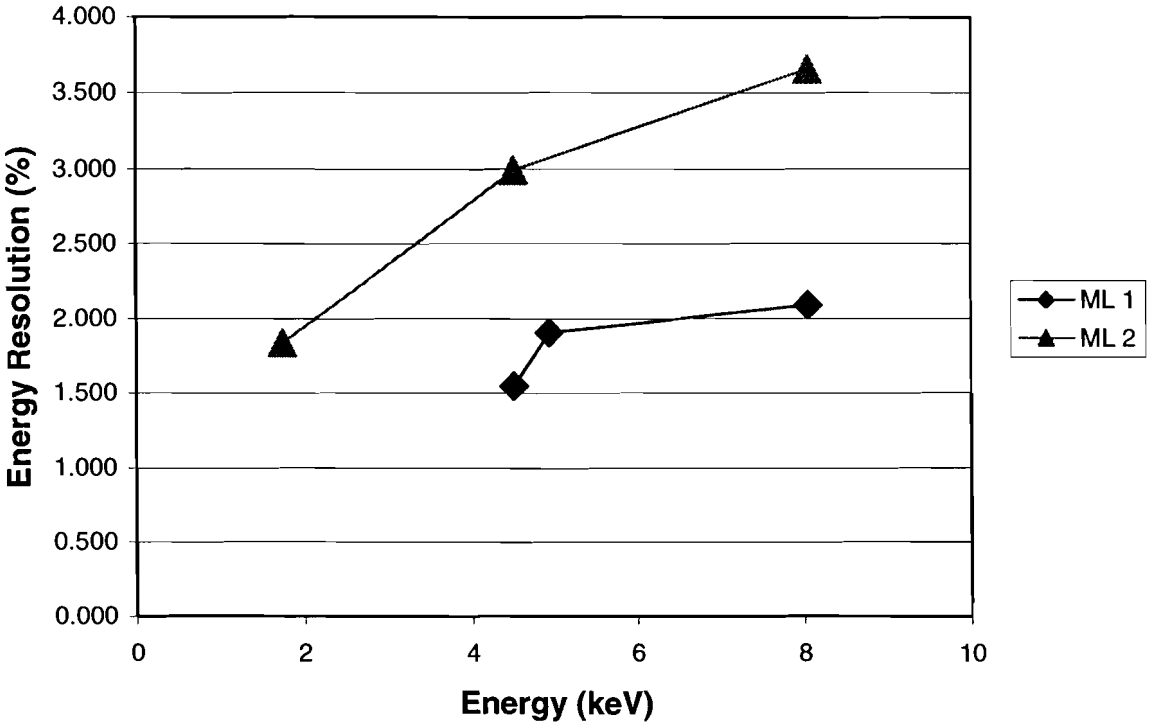

Fig 9. Energy Resolution as a function of energy for each multilayer

CONCLUSIONS

The WB_4C multilayer diffractors have been characterized as a function of x-ray energy by measuring their reflectivity as a function of angle using a Si PIN detector. Optimization using Gaussian curve fitting allows determination of the peak reflectivity as well as the energy resolution [full width at half maximum (FWHM)]. The multilayer spacing d is determined using Bragg's Law and the simultaneous analysis of multiple diffracted lines.

The first multilayer (d = 24.95 $\pm$0.3 Å) had a reflectivity of 40 to 70 % and an energy resolution of 1.5 to 2.1 %. The second multilayer (d = 36.3$\pm$0.74 Å) had a reflectivity of 32 to 89 % and an energy resolution of 1.8 to 3.7 %. The observed and calculated data can accurately be used as a foundation for further work with x-ray imaging using these multilayer diffractors.

Acknowledgements

I would like to acknowledge the support of the staff at the Laboratory for Laser Energetics of the University of Rochester. I would especially like to thank Dr. Frederic J. Marshall for his guidance and Robert Forties for his assistance in the completion of my project. I would also like to thank Dr. Stephen Craxton for allowing me to participate in this research program.

References

1. T.R. Boehly, D.L. Brown, R.S. Craxton et al., Opt. Commun. 133, 495 (1997).

2. Ahlstrom, H.G. Physics of Laser Fusion Vol. II: Diagnostics of Experiments on Laser Fusion Targets at LLNL. (Lawrence Livermore Laboratory, University of California, Livermore, CA, 1982), pp.2-9.

3. F. Ze, R.L. Kauffman, J.D. Kilkenny et al. Rev. Sci. Instrum. 63, 5125 (1992).

4. OSMIC, Inc. Auburn Hills, MI 48326.

5. AMPTEC, Inc. 6 DeAngelo Drive. Bedford, MA 01730

6. Cullity, B. D. Elements of X-Ray Diffraction. (Addison-Wesley Publishing Company, Inc., Reading, MA, 1956), pp. 78-103.

7. Cullity, ibid., pp. 17-23.

8. Knoll, Glenn F. Radiation Detection and Measurement. (John Wiley & Sons, New York, 1989), pp. 17-18.

9. Young, Hugh D. Statistical Treatment of Experimental Data. (McGraw-Hill Book Company, Inc., New York, 1962), pp. 64-76.

10. Visual Numerics, Inc. Houston, TX 77042.

11. Bevington, Philip. Data Reduction and Error Analysis for the Physical Sciences. (Mc Graw-Hill, New York, 1969)

12. M. Lampton, B. Margon, S. Bowyer. Astrophysical Journal. 208, 181 (1976).